A theoretical model of the endothelial cell morphology due to different waveforms

P. Sáez[a], M. Malve[b], M.A. Martínez[c,d]

[a] *Mathematical Institute, University of Oxford, Oxford, UK.*
[b] *Public University of Navarra, Department of Mechanical Engineering, Pamplona, Spain*
[c] *Applied Mechanics and Bioengineering. Aragón Institute of Engineering Research (I3A). University of Zaragoza. Zaragoza. Spain*
[d] *CIBER de Bioingeniería, Biomateriales y Nanomedicina (CIBER-BBN). Zaragoza. Spain*

Abstract

Endothelial cells are key units in the regulatory biological process of blood vessels. They represent an interface to transmit variations on the fluid dynamic changes. They are able to adapt its cytoskeleton, by means of microtubules reorientation and F-actin reorganization, due to new mechanical environments. Moreover, they are responsible for initiate a huge cascade of biological processes, such as the release of endothelins (ET-1), in charge of the constriction of the vessel and growth factors such as $\mathrm{TGF}-\beta$ and PDGF. Although a huge effort have been made in the experimental characterization and description of these two issues the computational modeling have not gain such a attention. In this work we propose a 3D model for cytoskeleton cells and a computational approach to, based on its mechanical environment, adapt or remodel its internal structure. We found our model fit with the experimental works presented before, both in the remodeling of the cell structure. We include our model within a computational fluid dynamic model in a carotid artery to quantify endothelial cell remodeling. Moreover, our approach can be coupled with models of collagen and smooth muscle cell growth, where remodeling and the associated release of chemical substance are involved.

Keywords: Endothelial cells, Remodeling, CFD

1. Introduction

Cells are the main trigger units controlling the mechanosensing in living tissue, and to do it so, they posses a complex apparatus. This is a very vast research field, see, among many others, the monographes of [49] and [3]. The complex mechanical study of cells can be split in two different approaches. A microscopical one, which describe changes on cells change, deformation and motility of the whole structure and the one comprising the internal behavior, which include its remodeling, sensing and signaling of mechano-chemical changes of the environment, leading to a wide cascade of events. Communication between cells ant its environment is regulated by intracellular signal molecules, receptor proteins, usually at the cell surface binding between them to activate the receptors and in turn relay the intracellular pathways which finaly activate the appropriate effector proteins, as ion channels, gene regulators proteins or remodeling of the cytoskeleton. Therefore, the study of cell mechanics can be approached from a macroscopic and microscopic point of view, as well as a pure mechanical or chemical approach. A common point between any kind of cell is its ability to sense its environment. This sensing machinery have been and is being extensively studied, although now yet well know.

It is well known that biological tissue remodels itself when driven by a given stimulus, e.g. mechanical loads such as an increase in blood pressure, and changes in the chemical environment that controls the signaling processes and the overall evolution of the tissue. Biological remodeling can occur in any kind of biological tissue. In particular, the study of collagen as the most important substance to be remodeled, in all its types (preferentially Type I and III), has been given considerable attention in the last few years [19, 39, 20]. The reorientation of this kind of structures can be assumed to be the consequence of the reorientation of the fibrils or filaments that make them up. This phenomenon leads to changes in the micro-structural orientation and fiber shape (due to the reorientation of the fibrils (see e.g. [56, 52, 55]). Several remodeling models have been proposed in recent years. Some of them analyze the reorientation of unidimensional fibers driven by different stimuli such as [45] or in a mcirosphere 3D approach [46, 62] or [35]. In [28], a complete consistent linearization of the equations in an implicit finite element framework was performed. [25] presented an elegant energetic and stationary study of the remodeling problem from a thermodynamic point of view.

Another important biological structure able to remodel itself is cell cytoskeleton. Cells move and reorient their inner structure depending on the stiffness and strain of the substrate [18, 16]. Cytoskeleton shape can change due to the adaptation of the microtubules and filaments to a specific external mechano-chemical stimulus [53, 17]. There are several experimental tests in the literature showing morphological changes of the cell due to mechanical stimulation of the matrix where cells are located.

In many cases this change of shape, unlike changes in orientation, are measured by a shape-index in the biomedical community. The underlying biological processes are more in number and complexity. Some of them, like dynamic of focal adhesions, the tension exerted by molecular motors over actin stress fibers are among the most important aspects to be considered (see e.g. [49] for an overall understanding of cell behavior). In reference to models capturing these features not much have been done while in terms of the orientation of the preferential direction of the cell, some of the most accepted models are those presented in [16, 15] where the reorientation is assumed to be controlled by the matrix behavior and the forces that arise from the active regulation of the cell in a dipole-like manner. In terms of modeling changes on the morphology of cell shape due to external stimuli no many models exists in the literature, see e.g. [40, 33, 50].

[7] showed that steady laminar flow and pulsating flow make EC to reorient in the direction of the flow and that the aspect ratio of the cells increase in a very similar fashion. [23] studied the structural organization of several elements of the cell (microfilaments, microtubules and intermediate filaments) also seeing that the main orientation of cell align in the direction of the flow. In similar studies [40] and [36] showed that in arterial coarctated model EC in the laminar zone before coarctation presented very tip-shapes while in the recirculation zone, after coarctation, EC showed a more random structure. [40] reported shape indexes (SI) of 0.2 for the laminar zones while turbulent flow induces SI from 0-4 to 1. [21] reported changes in the SI from 0.6 to 0.3-04. [41, 50] among others have shown this same behavior in their works. In a review article [10] resume some of the characteristic morphological changes due to different mechanical stimuli.

[14] presented a study pointing out that, although high shear stress in laminar flow promote cell alignment in the direction of the flow, low turbulent shear stress promote synthesis of endothelial DNA even in the absence of a organized structure of the cells suggesting that this type of flow is prone to develop atherome plaque and other diseases. Another feature of all these studies is the formation of stress fibers in the direction of the fluid for the laminar flow and in a random distribution in case of turbulent patterns. Stress fibers (see ,e.g., [49]) are important structural elements and their formation lead to changes in the mechanical behavior of the cell. However, we will ignore these phenomena in this study. In terms of modeling changes on the morphology of cell shape due to external stimuli no many models exists in the literature, see e.g. [40, 33, 50].

Introducing multi-scale approaches is a straightforward technique to take into account underlying evolving processes. The works of Ingber [34] about tensegrity models of cell structures is a good example in the field of cell mechanics. Microplane models were first used by [48] to study the micro-structural behavior of polymers. Later, [9] applied this approach, also known as microplane, for vascular tissue. In multi-scale homogenization schemes, the macroscopic behavior is recovered by averaging the micro-structural behavior represented, in the case of biological fibered tissue, by the mechanics of the fibrils or filaments. Previous authors [1] have used exponential-type models, such as that proposed by [29]. Recently [46] presented a microsphere-based approach for remodeling, where the fibrils behavior was modeled by the Worm-like Chain model (WLC).

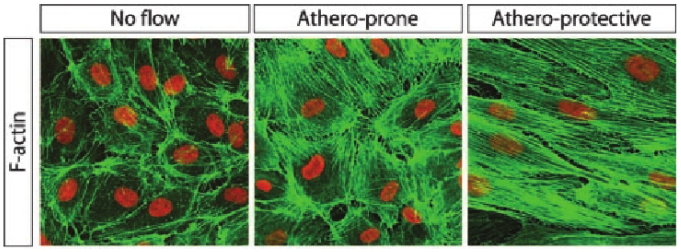

Figure 1: Cell morphology in a no-flow situation and athero-prone and protective flow condition reported by [13]© (© Copyright (2004) National Academy of Sciences, U.S.A.)

In short, we present a new remodeling model in 3D, taking into account the reorientation of the mean direction of a given fibered structure and the reorientation of the individual fibrils or filaments leading to changes in the parameters of the associated statistical orientation density function. We begin discussing the material model used and in particular the WLC model adopted for each fibril. Later, we present the Bingham statistical distribution, its main properties and general shape. We make use of the microsphere-based approach as homogenization technique to move from the micro to the macro-scale. In the following section, the evolution equation for remodeling are presented. We continue with the thermodynamic formulation of the problem obtaining the expression for the dissipation and a finite element case is carried out. To conclude the chapter, we applied the developed model to describe the adaptation process of endothelial cells (EC) to the mechanical stimuli exerted by the blood flow. In the subsequent section we discuss some examples to show the capabilities of our approach and we finish with a discussion of the advantages and limitations of the present contribution.

2. CFD simulation

The used patient-specific carotid geometry was reconstructed using computed tomography (CT) scans at one time point of the cardiac cycle. See [42] for a complete description of the geometry reconstruction and the CFD details. The complete segmented geometry considered in this study included the common carotid (CCA) and its principle branches: the internal carotid (ICA) and the external carotid (ECA). The intraluminal vessel wall was imported into the commercial software Ansys Icem CFD [58] for performing the computational mesh. A fully tetrahedral mesh

was generated by means of the aforementioned software using the well known Ansys Icem Octree algorithm. The final mesh had 10^6 elements, which was imported into the software package Ansys CFX v.14.5 [58] where the CFD simulation was performed.

The boundary conditions for the patient specific flow rates were not available for these subjects, so that the inlet and outlets flow rate waveforms were taken from literature. In particular, we used the averaged CCA, ECA and ICA waveform described by Lee et al. (2008) [59]. This waveforms were applied as flat profiles at the extremities of the computational model. In particular, 5-inlet nad 5-outlet diameter extensions, composed by prismatic three-dimensional grid elements, were added to the carotid artery in order to guarantee fully developed flow. No-slip conditions were finally imposed at the arterial walls.

The carotid blood flow was modeled as laminar, incompressible (density, ρ_f=1050 $\frac{Kg}{m^3}$) and non-Newtonian, using the Carreau constitutive law. The Carreau model assumes that the viscosity of blood, μ, varies according to the following equation:

$$\mu = \mu_\infty + (\mu_0 - \mu_\infty) \cdot (1 + A_c \dot{\gamma}_{ij}^2)^{m_c} \tag{1}$$

where μ_0 and μ_∞ are low and high shear rate asymptotic values, while the parameters A_c and m control the transition region size [60].The Carreau blood model predicts decreasing viscosity at high strain. For this study we used the experimental values provided in [60] and used also by other authors [61]: $\mu_0 = 0.056$ $\frac{N \cdot s}{m^2}$, $\mu_\infty = 0.00345$ $\frac{N \cdot s}{m^2}$ A_c=10.975 and m_c=-0.3216.

The Navier-Stokes equations, i.e., mass and momentum conservation were solved for unsteady, incompressible laminar flow by means of a finite volume discretization approach used by Ansys CFX [58]. The governing equations are solved simultaneously across all domain nodes by means of a cascade of successively coarser grids. this approach used by Ansys CFX allows the solution information to propagate rapidly across the computational domain. The linear set of equations that arises by applying the finite volume method to all elements in the domain results in a set of discrete conservation equations which can be solved through a coupled solver for the velocity field (cartesian components u, v, w) and the pressure term p as a single system.

This solution approach uses a fully implicit discretization method at any given time step. The linear equations are solved using an Algebraic Multigrid method. The Multigrid Linear Solver is an agglomeration-based and adaptively coarsened method which in a very effective manner is capable to solve the system of linearized equations. For this aim, the Ansys CFX Multigrid method adopts the so called factorization accelerated incomplete lower upper (ILU) technique for solving the discrete system of linearized equations written in linearised form as:

$$[A][\phi] = [b] \tag{2}$$

The ILU algorithm approaches the exact solution of the equations by means of several iterations starting from an approximate solution ϕ^n that is to be improved by a correction ϕ' obtaining a better solution ϕ^{n+1}:

$$\phi^{n+1} = \phi^n + \phi' \tag{3}$$

Repeated application of the aforementioned algorithm will yield the solution with the desired accuracy. The convergence criteria used in the simulation performed in this study was $1 \cdot 10^{-12}$. This factor was used to reduce the initial mass flow residual during the simulation progress. The computation was carried out using the 16 node, Dual Nehalem (64 bits), 16 processor cluster with a clock speed of 2.33 GHz and 32 Gb memory for each node.

3. Evolution equations for cell remodeling

The macroscopic part, *the micro-sphere-based anisotropic approach*, also known as micro-plane models, constitutes a homogenization technique that has been used previously for polymers [48] and biological tissue [2], among many other applications. The homogenization or continuous averaging $\langle(\bullet)\rangle$ of a given variable $(\bullet)$ is carried out by integrating over the unit sphere surface. In order to perform a numerical implementation, the integral is computed by addition on m discrete orientation vectors with the corresponding weight factors w^i as

$$\langle(\bullet)\rangle = \frac{1}{4\pi} \int_{\mathbb{U}^2} (\bullet) \mathrm{dA} \approx \sum_{i=1}^{m} w^i (\bullet)_i, \tag{4}$$

where dA is the differential area element of the unit sphere that may be written in terms of the spherical angles $\alpha \in [0, \pi)$ and $\phi \in [0, 2\pi)$ as $\mathrm{dA} = \sin(\alpha)\mathrm{d}\phi\mathrm{d}\alpha$. The normalizing term 4π is the unit sphere total area $A_{\mathbb{U}^2} = 4\pi$.

Although not considered here, at the micro-scale, *the behavior of the fibrils*, has been modeled previously modeled by the well-established WLC model [37]. The WLC was used in DNA modeling by [8]. Recently it was used by [24], [39] and [2], among others, to model the behavior of biological tissue, as an extension of the WLC molecular model to approach continuum tissue.

Here we use this geometrical approach to represent the structure of the cell. Although we are not introducing the mechanical behavior of the model, it could be recover by the homogenization described above. The reorientation of the fibrils or filaments that changes the shape can be identified in nature, e.g., with those processes discussed in the introduction section, such as rotations of cells like a dipole and a morphological change of its shape. We base our evolution equations on the reorientation process described by [44, 54, 57]. The realignment will be driven, at the moment, by a given general stimulus characterized by a second order tensor.

Some authors have modeled this phenomenon by means of the evolution of the statistical distributions [19, 20, 5]. [47] studied this issue by using a von Mises distribution and

the evolution of the associated structural tensor. Recently [46, 54] presented a work for remodeling within a micro-sphere approach, where from an initial isotropic state, the reorientation of each of the integration directions leads to an anisotropic behavior. This latter approach follows an approach similar to that described in [28] for one simple fiber, and is similar to the one used here for the evolution of the fibrils.

With such an approach, we are able to evolve the shape of the micro-structure by means of the evolution of each integration direction. From our point of view, this approach allows a more free reorientation of the fibrils since they do not have to be subject to fit with any statistical distribution. Future works will investigate the potential of options (i) and (ii).

We will follow the approach in [57]. It is necessary to define the vector $\boldsymbol{\omega}_i$, which leads the evolution of the reorientation process. As mentioned above, we prefer to generalize the driving quantity leading the process, named $\boldsymbol{\Xi}$. We assume that the realignment depends on the maximum principal direction of $\boldsymbol{\Xi}$, such that $\mathbf{r}_i \longmapsto \boldsymbol{\Xi}_3$. We will denote $\boldsymbol{\Xi}_3$ the eigenvector associated to maximum eigenvalues of $\boldsymbol{\Xi}$. This leads to

$$\boldsymbol{\omega}_i := \mathbf{r}_i \times \boldsymbol{\Xi}_3, \tag{5}$$

where $\boldsymbol{\omega}_i$ and $\mathbf{r}_i$ are the angular velocity and the unit vector of each integration direction. Incorporating Eq. 5 into $\dot{\mathbf{r}_i} = \boldsymbol{\omega}_i \times \mathbf{r}_i$ we obtain

$$\dot{\mathbf{r}_i} = [\mathbf{I} - \mathbf{r}_i \otimes \mathbf{r}_i] \cdot \boldsymbol{\Xi}_3. \tag{6}$$

However, we will again make use of the updating scheme presented in the section above, based on the exponential map, and again adopt an explicit updating ([43, 44]). We can also define $\omega_i = \|\boldsymbol{\omega}_i\|$, $\mathbf{n}_i^{\boldsymbol{\omega}_i} = \boldsymbol{\omega}_i/\omega_i$ and $\hat{\mathbf{n}}_i^{\boldsymbol{\omega}_i} = -\varepsilon \cdot \mathbf{n}_i^{\boldsymbol{\omega}_i}$. We approximate the updated vector as

$$\mathbf{r}_i^{n+1} = exp(\hat{\mathbf{n}}_i^{\boldsymbol{\omega}} \Delta t) \cdot \mathbf{r}_i^n. \tag{7}$$

As pointed out in the Introduction section, it is still unclear if this quantity is associated to strains or stresses variables (see e.g. reviews in [31, 12, 16, 57] and references therein). The driving quantity that will drive the remodeling is based on a magnitude-dependent parameter $\bar{\zeta}^{\boldsymbol{\Xi}}$ and the corresponding material dependent parameter $\bar{\zeta}_*^{\boldsymbol{\Xi}}$.

$$\bar{\zeta}^{\boldsymbol{\Xi}} = \begin{cases} 0 & \text{if} \quad \Lambda_3^{\boldsymbol{\Xi}}/\Lambda_1^{\boldsymbol{\Xi}} \leq \bar{\zeta}_0^{\boldsymbol{\Xi}} \\ \Lambda_3^{\boldsymbol{\Xi}}/\Lambda_1^{\boldsymbol{\Xi}} - \bar{\zeta}_0^{\boldsymbol{\Xi}} & \text{if} \quad \Lambda_3^{\boldsymbol{\Xi}}/\Lambda_1^{\boldsymbol{\Xi}} > \bar{\zeta}_0^{\boldsymbol{\Xi}} \end{cases}, \tag{8}$$

where $\boldsymbol{\Xi}$ denotes the driving quantity, $\Lambda_3^{\boldsymbol{\Xi}}/\Lambda_1^{\boldsymbol{\Xi}} \in [1, \inf)$ is the ratio between the maximum and minimum eigenvalues of the chosen driving quantity $\boldsymbol{\Xi}$ and $\zeta_0^{\boldsymbol{\Xi}}$ a threshold value that sets the coefficient value at which the reorientation process starts.

The updating scheme of Eq. 7 changes to

$$\mathbf{r}^{n+1} = exp(\bar{\zeta}^{\boldsymbol{\Xi}} \hat{\mathbf{n}}^{\boldsymbol{\omega}} \Delta t / \bar{\zeta}_*^{\boldsymbol{\Xi}}) \cdot \mathbf{r}^n. \tag{9}$$

4. Results: Application to the endothelial cell morphology

In this section we adapt the methodology developed previously to predict the morphological features of the EC in different zones of the carotid artery where EC align in the direction of the flow for laminar and high wall shear stress value. [13] studied experimentally this very same issue in a carotid artery based on two different waveforms, an athero-protective (related to high laminar shear stress) and a athero-prone waveform (related to recirculation in low wall shear stress). We can see the structure the cell organization in both types of situations in Fig. 1. The starting point of this approach consist of micro-sphere cell-like structures placed over the arterial lumen. The initial shape of the EC correspond with a orthotropic distribution, this is a cell with a round shape and structure with the orthotropic plane tangent to the surface of the lumen.

The morphological changes that we described above are simulated by means of the remodeling approach developed during the previous sections. We use the model described in 3. As we discussed, this approach describe a reorientation of the fibrils or filaments that make up such a structure. In this case the driving stimuli is the wall shear stress in the arterial lumen. The morphological changes will be based on the updating procedure described in Eq. 7.

The reorientation direction expressed before as $\boldsymbol{\Xi}_3$ is going to be given by the time average of the WSS, so

$$\boldsymbol{\Xi}_3 = \frac{1}{T} \int_0^t \boldsymbol{\tau}_w dt, \tag{10}$$

For the magnitude-dependent parameter $\bar{\zeta}^{\boldsymbol{\Xi}}$, we adopted the values of the time average wall shear stress (TAWSS) [63], defined as

$$\bar{\zeta}^{\boldsymbol{\Xi}} = \text{TAWSS} = \frac{1}{T} \int_0^t \|\boldsymbol{\tau}_w\| dt, \tag{11}$$

which represent the mean wall shear stress over the cardiac cycle period T, with time the time, and $\boldsymbol{\tau}_w$ is the wall shear stress.

The corresponding material dependent parameter $\bar{\zeta}_*^{\boldsymbol{\Xi}}$ is considered now a function of the Oscillatory Shear Index (OSI) [64],

$$\text{OSI} = 0.5 * \left[1 - \frac{\| \int_0^t \boldsymbol{\tau}_w dt \|}{\int_0^t \|\boldsymbol{\tau}_w\| dt} \right], \tag{12}$$

defined as $\bar{\zeta}_*^{\boldsymbol{\Xi}} = 1/\text{OSI}$. The OSI, variable that indicate the degree of variation in the direction of the flow, vary from 0 for a constant direction of the flow to 0.5 for a variation of 180 degrees in the direction of the flow. This is the reason for considering OSI as one of the parameters related to the remodeling on EC in blood flow conditions.

To measure the shape variation we compute the following structural tensor, $\boldsymbol{\rho}$, as

$$4\pi \boldsymbol{\rho}^n = \int_{\mathbb{U}^2} \rho(\mathbf{r}^n; \mathbf{Z}, \mathbf{Q}^n) \mathbf{r}^n \otimes \mathbf{r}^n \mathrm{dA}. \tag{13}$$

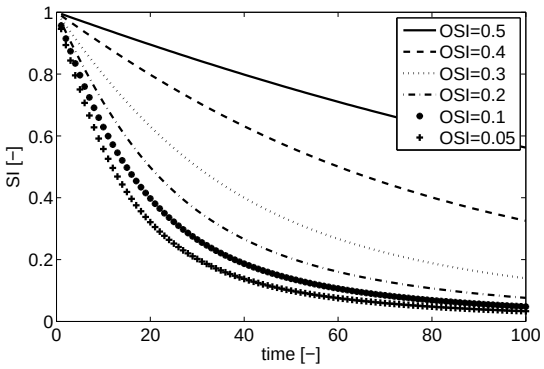

(a) Variation for different OSI at TAWSS=4Pa.

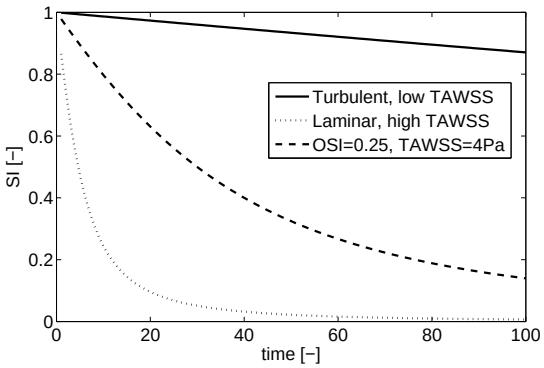

(b) Variations for extreme ranges of OSI and TAWSS.

Figure 2: Evolution of the SI for different types of the fluid characteristics.

This tensor provides a symmetric second order tensor, where initially two of the diagonal components are equal (since we start form an anisotropic distribution) and during the evolution process one of them turn to the unity and the other to zero. The ratio between these two values can be taken as the shape index factor, SI $= \rho_{33}/\rho_{22}$.

4.1. Benchmark results

We consider the range of OSI values [0-0.5] and the range of TAWSS [0-10] Pa to demonstrate the evolution capabilities of the model. We show in Fig. 2(a) the evolution of the SI for different values of OSI and a TAWSS of 4 Pa. In Fig. 2(b) we present the evolution of the SI for a OSI=0.5 and low TAWSS (TAWSS=1Pa), OSI=0.05 and high TAWSS (TAWSS=10) and a intermediate situation (OSI=0.2, TAWSS=5Pa).

We now reproduce the experimental results collected by [40] (Fig. 3), represent the evolution of the SI agains values of mean wall shear stress. Our simulations show very similar behavior, as we can see in Fig 3, with the experimental finding described previously.

4.2. CFD results

First we compute the CFD simulation as described in Section 2. The results of the TAWSS vector are shown in

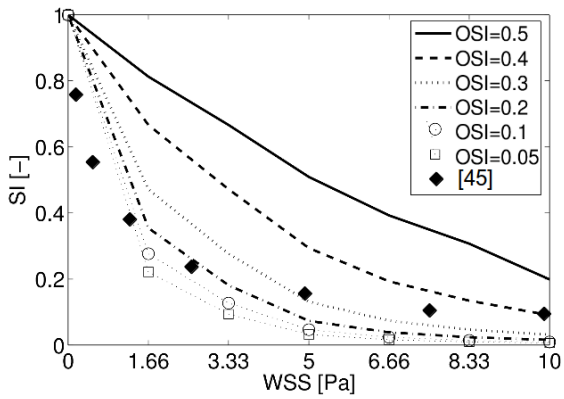

Figure 3: Evolution of the SI for different values WSS values for experimental data reported in [40] and the model presented here for different vaues of OSI.

Fig. 4 that we use as the main direction ($\mathbf{\Xi}_3$) of reorientation of the cells.

The values of OSI and TAWSS module are shown in Fig. 5.

Based on these results and the model at hand, we plot the results on the SI all over the surface of the carotid artery (see Fig. 6). We can see that zone with lower OSI produce a SI of 0.4-0.6. On zones where the OSI is close to 0 and the TAWSS is at the maximum SI rise up to values close to one. On the other side, OSI values around 0.4-0.5 and low TAWSS the SI goes down to values around 0-0.2, which represent very rounded structures.

In Fig. 7 we capture the evolution of the cell structure during the remodeling process. The figures, representing the microtubules coming from the centrosome, can be identified with the picture of the cell organization in Fig. 1. As the TAWSS for a given OSI, the strucutre of the cell become more slender. Similarly, as the OSI increase (from laminar to recirculation flow) at a given TAWSS the structure also turn into a more tip-like structure. This features are in agreement with the experimental observation described above.

5. Discussion

The adaptation of biological tissues has been a very active research field in recent years. In this contribution we have focused on the reorientation process of endothelial cell, proposing a complete 3D model that accounts for the reorientation the structure and the fibrils or filaments, in particular microtubules, that compose such a structure. In more general description of remodeling, most of the previous works have described the reorientation of a simple 1D fiber while, more recently, some others have taken into account the remodeling of the underlying structure by means of changes in its statistical distribution [5, 47]. Our goal was to develop a model to be capable of describing the distribution of the microstructure. We considered a

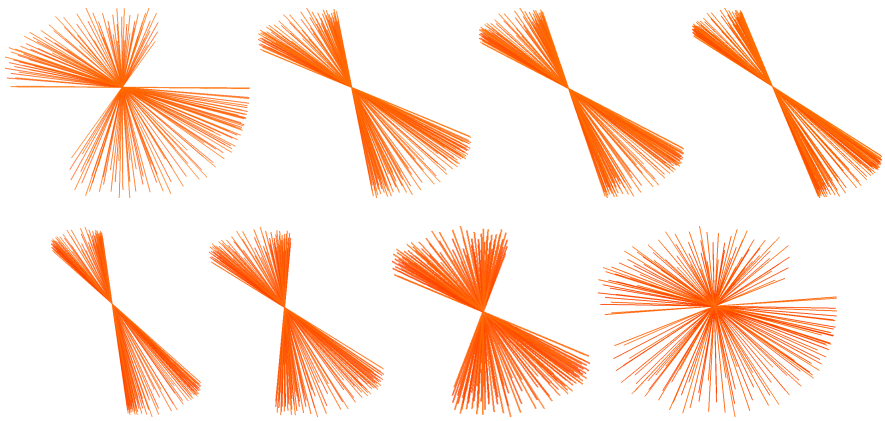

Figure 7: In the first row, evolution of the cell structure for different combination of TAWSS [0-10] with OSI=0.25. In the second row, evolution of the cell structure for different combination of OSI [0-0.5] with TAWSS=0.25. Values of OSI and TAWSS increasing from left to right.

microsphere-based model that allowed us to include this aspect of the problem. Numerous works have analyzed different types of driving quantities in these processes (see e.g. [39, 17, 5] and references therein), stress and strain being the most common for mechanical .

We exploit the option of modeling the adaptation of EC to the stimuli of the wall shear stress. The model was based on the remodeling of the micro-structure. Different flow features, as the TAWSS or the OSI, were considered as the driving forces to describe the remodeling process of the EC. The OSI, a measure of the variation of the direction of the flow, and the WSS are usual indicators of the cell morphology. Our simulation show that the SI of the cells under certain flow condition describe the actual morphology of EC in experimental data. The model represent a relatively simple view of the macroscopic remodeling of the cell structure.

The presented model has enormous capabilities for characterizing the evolution of complex biological fibered structures such as, for example, collagen bundles or cells. However there are certain limitations which need to be overcome in order to significantly improve it. The first, which does not apply only to our model, is the determination of those parameters related with the reorientation rate. For example, in a cell stretched by its substrate, tracking all the microtubules could help us to fit not only the material parameters but proposed driving quantities which would best fit such experiments. The theoretical and computational models would bring out an interesting mathematical description of these biological processes. The second drawback is the actual simplification onn the cell behavior and stucture. Cell are very complex structures where many chemical factores are also involve. We only consider the microtubules as thecontroling strutures to lok at the cell morpholgy. Other elements, as the stress fibers, could be included in further developments.

From our point of view, the most of future work would be focus on extending the model to the numerical simulation of more complex cell mechanics. For example, the amount and distribution of stress fibers generated due to a mechanical stimulus. Also to extend to different type of loads. There exists two main procedures to induce cell morphological changes, static and cyclic loading [16, 26]. While static and low-frequency loading leads to a reorientation and remodeling of the cellular structure parallel to the stretching direction [11, 6], high-frequency cyclic loading does in nearly perpendicular [27, 30, 22]. Looking at these different type of loads will be also a future key point of research. It is also know that the remodeling of EC lead to the formation of atherome plaque. More complex CFD, or FSI simulation to coupling the fluid behavior with the deformation of a substrate, could also be an interesting ongoing work to look at the effect of both mechanical effects and other biological aspects [65, 66]. Our model could be used to study , e.g., the synthesizing of different substances related to the EC adaptation, setting the morphological changes of EC as the trigger factor.

In short, we have extended a 3D reorientation model for endothelial cells. We have used an exact updating scheme for these reorientations, considering the flow features as the main drving forces of the remodeling process. This approach allows to model different remodeling processes in biological tissues, and with the appropriate experiments could lead to a better knowledge of how biological tissue adapts to its specific environment. Combined with the development of a growth model (see [32, 4]) our approach could help modeling and predicting the overall behavior of tissue reacting to external stimuli, via the reorientation and growth (positive or negative), of its microstructure. We believe it have been and will represent a challenging area of research.

6. Bibliography

[1] V. Alastrue, P. Saez, M. A. Martinez, and M. Doblare. On the use of the bingham statistical distribution in microsphere-based constitutive models for arterial tissue. *Mech Res Commun*, 37 (8):700–706, December 2010.

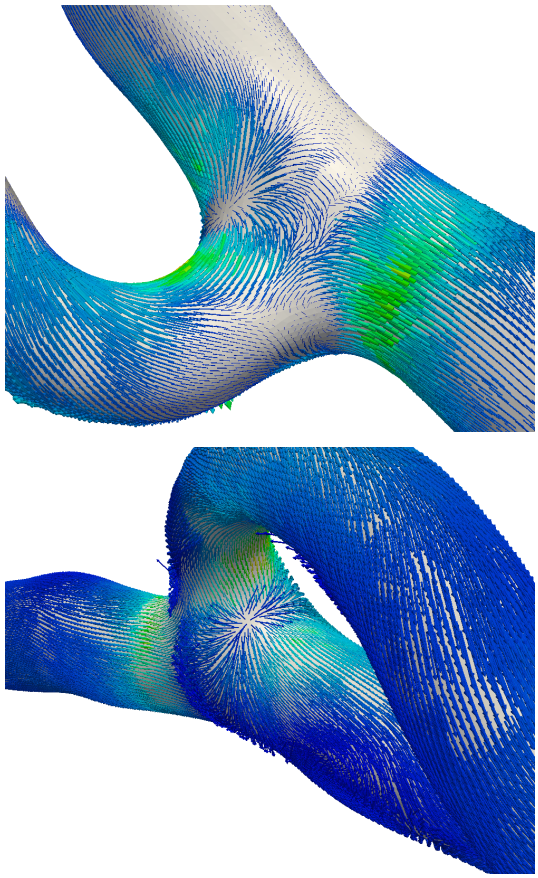

Figure 4: Different views of the TAWSS vector on the endothelium surface.

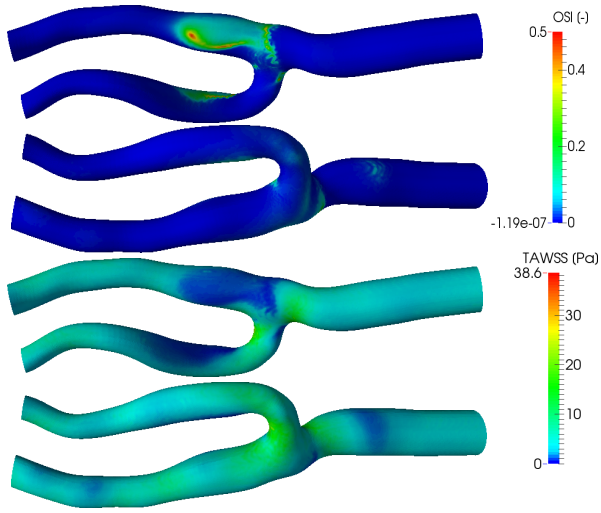

Figure 5: OSI and TAWSS in the carotid artery.

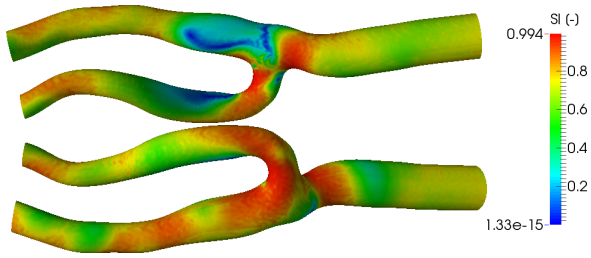

Figure 6: SI values in the carotid artery.

[2] V. Alastrué, M. A. Martinez, M. Doblare, and A. Menzel. Anisotropic micro-sphere-based finite elasticity applied to blood vessel modelling. *J Mech Phys Solids*, 57(1):178–203, January 2009.

[3] A. Alberts, A. Johnson, J. Lewis, M. Raff, K. Roberts, and P. Walter. *Molecular Biology of The Cell*. Garland Science, 2002.

[4] D. Ambrosi, G. A. Ateshian, E. M. Arruda, S. C. Cowin, J. Dumais, A. Goriely, G. A. Holzapfel, J. D. Humphrey, R. Kemkemer, E. Kuhl, J. E. Olberding, L. A. Taber, and K. Garikipati. Perspectives on biological growth and remodeling. *J Mech Phys Solids*, 59(4):863–883, April 2011.

[5] F. Baaijens, C. Bouten, and N. Driessen. Modeling collagen remodeling. *J Biomech*, 43(1):166–175, January 2010.

[6] I. B. Bischofs and U. S. Schwarz. Cell organization in soft media due to active mechanosensing. *Proceedings of the National Academy of Sciences of the United States of America*, 100(16): 9274–9279, August 2003. doi: 10.1073/pnas.1233544100.

[7] B. R. Blackman, G. Garcia-Cardena, and M. A. Gimbrone. A new in vitro model to evaluate differential responses of endothelial cells to simulated arterial shear stress waveforms. *J Biomech Eng-T ASME*, 124(4):397–407, August 2002. doi: 10.1115/1.1486468.

[8] Carlos Bustamante, Zev Bryant, and Steven B. Smith. Ten years of tension: single-molecule DNA mechanics. *Nature*, 421 (6921):423–427, January 2003. ISSN 0028-0836.

[9] Ferhun C. Caner and Ignacio Carol. Microplane constitutive model and computational framework for blood vessel tissue. *J Biomech Eng*, 128(3):419–427, June 2006.

[10] Shu Chien. Mechanotransduction and endothelial cell homeostasis: the wisdom of the cell. *Am J Physiol Heart Circ Physiol*, 292(3):H1209–1224, 2007.

[11] A. M. Collinsworth, C. E. Torgan, S. N. Nagda, R. J. Rajalingam, W. E. Kraus, and G. A. Truskey. Orientation and length of mammalian skeletal myocytes in response to a unidirectional stretch. *Cell and Tissue Research*, 302(2):243–251, November 2000. doi: 10.1007/s004410000224.

[12] S. C. Cowin. Tissue growth and remodeling. *Annu Rev Biomed Eng*, 6:77–107, 2004.

[13] G. H. Dai, M. R. Kaazempur-Mofrad, S. Natarajan, Y. Z. Zhang, S. Vaughn, B. R. Blackman, R. D. Kamm, G. Garcia-Cardena, and M. A. Gimbrone. Distinct endothelial phenotypes evoked by arterial waveforms derived from atherosclerosis-susceptible and -resistant regions of human vasculature. *Proc Nat Acad Sci USA*, 101(41):14871–14876, October 2004.

[14] P. F. Davies, A. Remuzzi, E. J. Gordon, C. F. Dewey, and M. A. Gimbrone. Turbulent fluid shear-stress induces vascular endothelial-cell turnover invitro. *Proc Nat Acad Sci USA*, 83 (7):2114–2117, April 1986. doi: 10.1073/pnas.83.7.2114.

[15] R. De and S. A. Safran. Dynamical theory of active cellular response to external stress. *Phys Rev E*, 78(3):031923, September 2008.

[16] R. De, A. Zemel, and S. A. Safran. Dynamics of cell orientation. *Nat Phys*, 3(9):655–659, September 2007.

[17] R. De, A. Zemel, and S. A. Safran. Do cells sense stress or strain? measurement of cellular orientation can provide a clue. *Biophys J*, 94(5):L29–L31, March 2008.

[18] D. E. Discher, P. Janmey, and Y. L. Wang. Tissue cells feel and respond to the stiffness of their substrate. *Science*, 310(5751): 1139–1143, November 2005.

[19] N. J. B. Driessen, G. W. M. Peters, J. M. Huyghe, C. V. C. Bouten, and F. P. T. Baaijens. Remodelling of continuously distributed collagen fibres in soft connective tissues. *J Biomech*, 36(8):1151–1158, August 2003.

[20] N. J. B. Driessen, M. A. J. Cox, C. V. C. Bouten, and F. P. T. Baaijens. Remodelling of the angular collagen fiber distribution in cardiovascular tissues. *Biomech Model Mechan*, 7(2):93–103, April 2008.

[21] M. A. Farcas, L. Rouleau, R. Fraser, and R. L. Leask. The development of 3-d, in vitro, endothelial culture models for the study of coronary artery disease. *Biomedical Engineering Online*, 8:30, October 2009. doi: 10.1186/1475-925X-8-30.

[22] U. Faust, N. Hampe, W. Rubner, N. Kirchgessner, S. Safran, B. Hoffmann, and R. Merkel. Cyclic stress at mhz frequencies aligns fibroblasts in direction of zero strain. *Plos One*, 6(12): e28963, December 2011. doi: 10.1371/journal.pone.0028963.

[23] C. G. Galbraith, R. Skalak, and S. Chien. Shear stress induces spatial reorganization of the endothelial cell cytoskeleton. *Cell Motil Cytoskel*, 40(4):317–330, 1998.

[24] K. Garikipati, H. Narayanan, E. M. Arruda, K. Grosh, and S. Calve. Material forces in the context of biotissue remodelling. In P. Steinmann and G. A. Maugin, editors, *Mechanics of Material Forces*. Springer, New York, 2005.

[25] K. Garikipati, J.E. Olberding, H. Narayanan, E.M. Arruda, K. Grosh, and S. Calve. Biological remodelling: Stationary energy, configurational change, internal variables and dissipation. *J Mech Phys Solids*, 54(7):1493–1515, July 2006.

[26] Z. Goli-Malekabadi, M. Tafazzoli-Shadpour, M. Rabbani, and M. Janmaleki. Effect of uniaxial stretch on morphology and cytoskeleton of human mesenchymal stem cells: static vs. dynamic loading. *Biomedizinische Technik*, 56(5):259–265, October 2011.

[27] K. Hayakawa, N. Sato, and T. Obinata. Dynamic reorientation of cultured cells and stress fibers under mechanical stress from periodic stretching. *Exp Cell Res*, 268(1):104–114, August 2001.

[28] G. Himpel, A. Menzel, E. Kuhl, and P. Steinmann. Time-dependent fibre reorientation of transversely isotropic continua . finite element formulation and consistent linearization. *Intl J Numer Meth Eng*, 73(10):1413–1433, March 2008.

[29] G. A. Holzapfel, T. C. Gasser, and R. W. Ogden. A new constitutive framework for arterial wall mechanics and a comparative study of material models. *J Elasticity*, 61(1):1–48, July 2000.

[30] H. J. Hsu, C. F. Lee, and R. Kaunas. A dynamic stochastic model of frequency-dependent stress fiber alignment induced by cyclic stretch. *Plos One*, 4(3):e4853, March 2009. doi: 10.1371/journal.pone.0004853.

[31] J. D. Humphrey. Stress, strain, and mechanotransduction in cells. *J Biomech Eng*, 123(6):638–641, December 2001.

[32] J. D. Humphrey. Need for a continuum biochemomechanical theory of soft tissue and cellular growth and remodeling. In *Biomechanical Modelling at the Molecular, Cellular and Tissue Levels*. Springer Vienna, 2009.

[33] D. E. Ingber. Tensegrity i. cell structure and hierarchical systems biology. *Journal of Cell Science*, 116(7):1157–1173, April 2003. doi: 10.1242/jcs.0359.

[34] D. E. Ingber. Tensegrity-based mechanosensing from macro to micro. *Progress In Biophysics & Molecular Biology*, 97(2-3): 163–179, June 2008. doi: 10.1016/j.pbiomolbio.2008.02.005.

[35] I. Karsaj, C. Sansour, and J. Soric. The modelling of fibre reorientation in soft tissue. *Biomech Model Mechan*, 8(5):359–370, October 2009.

[36] D. W. KIM, A. I. GOTLIEB, and B. L. LANGILLE. Invivo modulation of endothelial-f-actin microfilaments by experimental alterations in shear-stress. *Arteriosclerosis*, 9(4):439–445, July 1989.

[37] O. Kratky and G. Porod. Rontgenuntersuchung geloster fadenmolekule. *Recl Trav Cnim Pay B*, 68(12):1106–1122, 1949.

[38] E. Kuhl, P. Steinmann, and I. Carol. A thermodynamically consistent approach to microplane theory. part ii. dissipation and inelastic constitutive modeling. *Int J Solids Struct*, 38(17): 2933–2952, April 2001.

[39] E. Kuhl, K. Garikipati, E. M. Arruda, and K. Grosh. Remodeling of biological tissue: Mechanically induced reorientation of a transversely isotropic chain network. *J Mech Phys Solids*, 53 (7):1552–1573, July 2005.

[40] M. J. Levesque, D. Liepsch, S. Moravec, and R. M. Nerem. Correlation of endothelial-cell shape and wall shear-stress in a stenosed dog aorta. *Arteriosclerosis*, 6(2):220–229, March 1986.

[41] A. M. Malek and S. Izumo. Mechanism of endothelial cell shape change and cytoskeletal remodeling in response to fluid shear stress. *J Cell Sci*, 109:713–726, April 1996.

[42] M. Malve, S. Chandra, A. García, A. Mena, M. A. Martínez, E. A. Finol, and M. Doblaré. Impedance-based outflow boundary conditions for human carotid haemodynamics. *Comput Meth Biomech Biomed Eng*, DOI:10.1080/10255842.2012.744396, 2014. doi: 10.1080/10255842.2012.744396.

[43] J. E. Marsden and T. S. Ratiu. *Introduction to Mechanics and Symmetry: A Basic Exposition of Classical Mechanical Systems*. Springer Verlag, 1999.

[44] A. Menzel. Modelling of anisotropic growth in biological tissues. *Biomech Model Mechan*, 3(3):147–171, March 2004.

[45] A. Menzel. A fibre reorientation model for orthotropic multiplicative growth. *Biomech Model Mechan*, 6:303–320, 2007.

[46] A. Menzel and T. Waffenschmidt. A microsphere-based remodelling formulation for anisotropic biological tissues. *Phil Trans R Soc A*, 367(1902):3499–3523, September 2009.

[47] A. Menzel, M. Harrysson, and M. Ristinmaa. Towards an orientation-distribution-based multi-scale approach for remodelling biological tissues. *Comput Meth Biomech Biomed Eng*, 11(5):505–524, 2008.

[48] C. Miehe, S. Göktepe, and F. Lulei. A micro-macro approach to rubber-like materials–part i: the non-affine micro-sphere model of rubber elasticity. *J Mech Phys Solids*, 52(11):2617–2660, November 2004.

[49] M.R. K. Mofrad and R D. Kamm. *Cytoskeletal Mechanics - Models and Measurements*. Cambridge University Press, 2006.

[50] T. Ohashi and M. Sato. Remodeling of vascular endothelial cells exposed to fluid shear stress: experimental and numerical approach rid a-5424-2012. *Fluid Dynamics Research*, 37(1-2): 40–59, July 2005. doi: 10.1016/j.fluiddyn.2004.08.005.

[51] U. Olgac, V. Kurtcuoglu, and D. Poulikakos. Computational modeling of coupled blood-wall mass transport of ldl: effects of local wall shear stress. *American Journal of Physiology-heart and Circulatory Physiology*, 294(2):H909–H919, February 2008. doi: 10.1152/ajpheart.01082.2007.

[52] M. P. Rubbens, A. Driessen-Mol, R. A. Boerboom, M. M. J. Koppert, H. C. van Assen, B. M. T. Romeny, F. P. T. Baaijens, and C. V. C. Bouten. Quantification of the temporal evolution of collagen orientation in mechanically conditioned engineered cardiovascular tissues. *Ann Biomed Eng*, 37(7):1263–1272, July 2009.

[53] A. Saez, A. Buguin, P. Silberzan, and B. Ladoux. Is the mechanical activity of epithelial cells controlled by deformations or forces? *Biophys J*, 89(6):L52–L54, December 2005.

[54] P. Saez, E. Pena, M. Doblare, and M. A. Martinez. An anisotropic microsphere-based approach for fiber orientation adaptation in soft tissue. *Ieee Transactions On Biomedical Engineering*, 58(12):3500–3503, December 2011. doi: 10.1109/TBME.2011.2166154.

[55] E. A. Sander, T. Stylianopoulos, R. T. Tranquillo, and V. H. Barocas. Image-based multiscale modeling predicts tissue-level and network-level fiber reorganization in stretched cell-compacted collagen gels. *PNAS*, 106(42):17675–17680, October 2009.

[56] D. Stopak and A. K. Harris. Connective-tissue morphogenesis by fibroblast traction .1. tissue-culture observations. *Dev Biol*, 90(2):383–398, 1982.

[57] P. Sáez, E. Peña, M. Doblaré, and M.A. Martínez. Hierarchical micro-adaptation of biological structures by mechanical stimuli. *International Journal of Solids and Structures*, 50(1415):2353–2370, July 2013. ISSN 0020-7683.

[58] Ansys (2010) CFX Theory User Manual. Canonsburg, PA: Ansys Software.

[59] Lee SW, Antiga L, Spence JD, Steinman DA. 2008. Geometry of the carotid bifurcation predicts its exposure to disturbed flow.

Stroke. 39:2341–2347.

[60] B. Johnston, R. Johnston, S. Corney, D. Kilpatrick, Non-newtonian blood flow in human right coronary arteries: Transient simulations, Journal of Biomechanics 39 (2006) 1116–1128.

[61] A Valencia F Baeza, Numerical simulation of Fluid-Structure Interaction in stenotic arteries considering two layer nonlinear anisotropic structural mode,l International Communications in Heat and Mass Transfer, 2009, 36:137–142.

[62] T. Waffenschmidt, A. Menzel, and E. Kuhl. Anisotropic density growth of bone - a computational microsphere approach. *Int J Solids Struct*, 49:1928–1946, 2012.

[63] D. N. Ku, D. P. Giddens, C. K. Zarins, and S. Glagov. Pulsatile flow and atherosclerosis in the human carotid bifurcation. positive correlation between plaque location and low oscillating shear stress. *Arteriosclerosis*, 5(3):293–302, 1985.

[64] Heather A Himburg, Deborah M Grzybowski, Andrew L Hazel, Jeffrey A LaMack, Xue-Mei Li, and Morton H Friedman. Spatial comparison between wall shear stress measures and porcine arterial endothelial permeability. *Am J Physiol Heart Circ Physiol*, 286(5):H1916–H1922, May 2004.

[65] Diego Gallo, David A Steinman, Payam B Bijari, and Umberto Morbiducci. Helical flow in carotid bifurcation as surrogate marker of exposure to disturbed shear. *J Biomech*, 45(14):2398–2404, Sep 2012. doi: 10.1016/j.jbiomech.2012.07.007.

[66] Umberto Morbiducci, Raffaele Ponzini, Matteo Nobili, Diana Massai, Franco Maria Montevecchi, Danny Bluestein, and Alberto Redaelli. Blood damage safety of prosthetic heart valves. shear-induced platelet activation and local flow dynamics: a fluid-structure interaction approach. *J Biomech*, 42(12):1952–1960, Aug 2009. doi: 10.1016/j.jbiomech.2009.05.014.